Article

Discovery Medicine 2026; 38(208): 1661–1672
https://doi.org/10.24976/Discov.Med.202638208.130

Esketamine Protects Against Sepsis-Induced Intestinal Injury by Modulating Macrophage Polarization Through the TLR4/NF-κB Signaling Pathway

Liyan Miao[1], Li Zhang[1], Min Zhou[1], Qiuchun Chen[2,*]

[1]Department of Anesthesiology, Fujian Maternity and Child Health Hospital, College of Clinical Medicine for Obstetrics & Gynecology and Pediatrics, Fujian Medical University, 350001 Fuzhou, Fujian, China
[2]Department of Anesthesiology, Fujian Medical University Union Hospital, 350001 Fuzhou, Fujian, China
*Correspondence: aimazui1818@163.com (Qiuchun Chen)
Submitted: 23 October 2025 Revised: 5 March 2026 Accepted: 11 March 2026 Published: 20 May 2026

Background: Sepsis-induced intestinal injury plays a pivotal role in the progression of sepsis and multiple organ dysfunction syndrome (MODS). This study aimed to investigate the protective effects of Esketamine (ESK) on sepsis-induced intestinal injury, focusing on the modulation of inflammation, oxidative stress, and macrophage polarization via the Toll-like receptor (TLR)4/NF-κB signaling pathway. Additionally, *in vitro* studies were conducted to further elucidate the molecular mechanisms underlying ESK's effects on macrophage polarization.

Methods: A rat model of sepsis was established using the cecal ligation and puncture (CLP) method. ESK was administered at doses of 30 mg/kg and 60 mg/kg. Serum levels of pro-inflammatory cytokines (IL-1β, IL-6, TNF-α) were measured using ELISA, and histopathological analyses were performed on intestinal tissues to evaluate injury. TLR4/NF-κB pathway markers were assessed using Western blotting and qPCR analyses. *In vitro*, RAW 264.7 macrophages were treated with lipopolysaccharide (LPS) to induce sepsis-like conditions, followed by ESK treatment. Immunofluorescence staining and flow cytometry were used to evaluate macrophage polarization, focusing on M1 markers (CD86, iNOS) and M2 markers (Arg1, CD206).

Results: ESK treatment significantly ameliorated sepsis-induced intestinal injury *in vivo*. It reduced serum levels of pro-inflammatory cytokines while increasing the anti-inflammatory cytokine IL-10 compared to the CLP rats ($p < 0.05$). ESK also promoted M2 macrophage polarization (increased Arg1 and CD206 expression) and inhibited M1 macrophage polarization (decreased CD86 and iNOS expression) compared to the CLP rats ($p < 0.05$). *In vitro*, ESK demonstrated similar effects in LPS-stimulated RAW 264.7 cells, modulating macrophage polarization by inhibiting the TLR4/NF-κB signaling pathway compared to the LPS-stimulated cells ($p < 0.05$). Co-treatment with a TLR4 agonist abrogated these effects, confirming the involvement of TLR4 in the mechanism of action of ESK.

Conclusion: ESK protects against sepsis-induced intestinal injury by modulating macrophage polarization and suppressing inflammation through the TLR4/NF-κB signaling pathway. Both *in vivo* and *in vitro* studies demonstrated ESK's ability to shift macrophages towards an anti-inflammatory M2 phenotype, highlighting its potential as a therapeutic agent for sepsis management. This study first investigated the effects of ESK on sepsis-induced intestinal damage and the potential molecular mechanisms involved.

Keywords: sepsis; macrophage polarization; TLR4/NF-κB; intestinal injury

Introduction

Sepsis, characterized as a systemic inflammatory response syndrome (SIRS) triggered by infection, remains a significant challenge in critical care due to its persistently high mortality rate [1,2]. Recent research has increasingly underscored the pivotal role of the intestine in the pathogenesis and progression of sepsis [3,4]. Specifically, the intestine plays a central role in the transition from SIRS to severe complications, such as septic shock, acute respiratory distress syndrome (ARDS), and multiple organ dysfunction syndrome (MODS), making it a "trigger organ" for MODS [5–7]. Accordingly, protecting the intestinal barrier during the early stages of sepsis, while minimizing bacterial translocation, endotoxin absorption, and the release of inflammatory mediators, is critical for reducing the risk of multiple organ failure.

Macrophages are recognized as key mediators in the development of sepsis-induced intestinal injury [8, 9]. These immune cells can polarize into two distinct phenotypes with divergent functions: M1 and M2 macrophages. M1 macrophages are primarily associated with pro-inflammatory responses and are characterized by their production of inflammatory cytokines essential for

pathogen defense [10]. Conversely, M2 macrophages promote anti-inflammatory responses and tissue repair, facilitating the resolution of inflammation and promoting recovery [5,11]. Thus, regulating macrophage polarization is emerging as a crucial therapeutic strategy in mitigating sepsis-induced intestinal injury. A central regulator of macrophage polarization is the Toll-like receptor (TLR) family, particularly TLR4. TLR4 recognizes lipopolysaccharide (LPS), a major component of Gram-negative bacterial cell walls, and activates downstream signaling pathways, including the NF-κB pathway, which drives M1 macrophage polarization [12–14]. This process initiates a robust pro-inflammatory response. Importantly, TLR4 activation not only induces the release of multiple inflammatory cytokines but also upregulates its own expression, establishing a positive feedback loop that amplifies the inflammatory response [15–17]. Persistent activation of this loop exacerbates inflammation and can lead to multiple organ dysfunction. Therefore, targeting the TLR4/NF-κB signaling axis represents a promising therapeutic approach for shifting macrophage polarization toward the anti-inflammatory M2 phenotype, thereby attenuating inflammation and promoting intestinal recovery in septic patients.

In recent years, Esketamine (ESK), the S-enantiomer of ketamine, has garnered attention due to its broad utility in perioperative and ICU settings [18]. Its rapid onset of action, minimal respiratory depression, and versatility in administration routes make it an ideal agent for sedation and analgesia [19]. Beyond these established roles, emerging evidence suggests that ESK may confer organ-protective effects in the context of sepsis [20]. For instance, studies have demonstrated that ketamine can alleviate endotoxin-induced acute lung injury and ameliorate myocardial damage in septic animal models [21,22]. These protective effects are thought to be mediated, at least in part, through the modulation of inflammatory pathways. Specifically, ketamine has been shown to influence the TLR4/NF-κB signaling axis, a critical regulator of inflammation during sepsis, which may subsequently affect macrophage polarization [23]. By shifting macrophage polarization from the pro-inflammatory M1 phenotype toward the anti-inflammatory M2 phenotype, ESK may mitigate systemic inflammation and facilitate tissue recovery.

Despite the promising potential, ESK's specific effects on sepsis-induced intestinal injury and the underlying molecular mechanisms remain inadequately understood and require further investigation. To address this gap, the present study was the first to examine whether ESK mitigates sepsis-induced intestinal injury by modulating macrophage polarization through the TLR4/NF-κB signaling pathway. By elucidating the molecular mechanisms involved, this research seeks to provide critical experimental evidence to inform and enhance clinical strategies for managing sepsis- associated acute intestinal injury.

Methods

Animals

Eighty healthy adult male Sprague–Dawley rats, aged 8–10 weeks and weighing 230–270 g, were provided by the Laboratory Animal Center of Fujian Medical University. The protocol was approved by the ethical committee of Fujian Medical University (No. 2023-0131). The study was designed and ethically approved at Fujian Medical University, with additional experiments conducted at Fujian Maternity and Child Health Hospital due to specialized facilities available for tissue analysis. Rats were housed individually in ventilated cages under standard laboratory conditions: 12-hour light/dark cycles at a controlled ambient temperature of 22–25 °C, with free access to food and water except during fasting periods.

Establishment of Septic ALI Model

A total of 80 male Sprague-Dawley (SD) rats, weighing (240 $\pm$ 15) g, were obtained from Beijing Vital River Laboratory Animal Technology Co., Ltd. (Beijing, China). They were randomly assigned to four groups (n = 20 per group) using a random number table: Sham group: Rats underwent a sham operation without cecal ligation and puncture (CLP); CLP group: Rats underwent the CLP procedure but received no pharmacological treatment; CLP + ESK (CAS 33795-24-3; product No. K1884, Sigma-Aldrich, St. Louis, MO, USA) 30 mg/kg group: Rats received an intraperitoneal injection of ESK (30 mg/kg) 30 minutes after the CLP procedure; CLP + ESK 60 mg/kg group: Rats received an intraperitoneal injection of ESK (60 mg/kg) 30 minutes after the CLP procedure. ESK doses were selected based on previous studies [13,20]. In the Sham and CLP groups, an equivalent volume of 0.9% saline was injected intraperitoneally at the same time points to serve as control treatments. All rats were housed under a 12-hour light/dark cycle at an ambient temperature of 22–25 °C. The rats were individually housed and acclimatized to the laboratory environment for 10 days prior to the experiment. One percent sodium pentobarbital (50 mg/kg) was injected intraperitoneally to anesthetize the rats. After disinfection, the abdomen was incised 1 cm at the midline to expose the cecum. Silk thread was subsequently used to ligate the proximal third of the cecum and then punctured once with a 22-G needle, and fecal matter was extruded. Finally, the cecum was inserted back into the abdomen, and the incision was sutured. After surgery, 4 mL/100 g of normal saline was injected subcutaneously for fluid resuscitation.

In addition, bupivacaine (1 mg/kg; Cat. No. B5274, Sigma-Aldrich, USA) and butorphanol tartrate (0.05 mg/kg; Cat. No. 1082504, Sigma-Aldrich, USA) were used for postoperative analgesia. For rats in the sham groups, the cecum was only exposed and then returned to the abdomen. For each group, 10 rats were randomly selected for postoperative observation and mortality assess-

ment, while the other 10 rats' serum and intestinal tissues were collected 14 days after the treatment for subsequent experiments. Rats were euthanized at the end of the experiment using a two-step method in accordance with the AVMA Guidelines for the Euthanasia of Animals (2020) and the approved animal protocol. First, animals were placed in a transparent acrylic induction chamber (30 × 20 × 15 cm) connected to a calibrated vaporizer. They were deeply anesthetized with 5% isoflurane (NDC 10019-773-40, Baxter Healthcare, USA) delivered in 100% medical-grade oxygen at 1 L/min for approximately 2–3 min. The depth of anesthesia was rigorously confirmed by the complete absence of both the pedal withdrawal reflex (assessed by a firm toe pinch applied to a hind limb) and the corneal reflex (evaluated by gentle touching of the cornea with a sterile cotton swab). Once unresponsive, the rat was promptly removed from the chamber. Secondary euthanasia was immediately performed by rapid cervical dislocation, where the base of the skull was firmly grasped while the body was extended to ensure severance of the spinal cord from the brainstem. Death was confirmed by performing a bilateral thoracotomy to expose the heart, followed by visual verification of cardiac arrest and absence of respiratory movements for more than 1 min. All procedures complied with the ARRIVE Guidelines 2.0.

Postoperative Observation and Mortality

Postoperative monitoring of 40 male SD rats included body weight (±0.1 g), rectal temperature (ThermoWorks® probe, ±0.1 °C), and fecal/urine output, with mortality tracked for 14 days post-CLP. Humane endpoints requiring immediate euthanasia comprised: ≥20% weight loss sustained over 48 h, hypothermia <34 °C unresponsive to warming, neurological impairment preventing feeding, or ulceration affecting >15% body surface area.

Collection and Processing of Serum and Tissue Samples

Fourteen days post-treatment, rats (sacrifice weight: 252 ± 18 g; preoperative: 240 ± 15 g) were placed in an induction chamber and deeply anesthetized with 5% isoflurane in 100% oxygen (flow rate 1 L/min). Anesthesia depth was confirmed by the absence of pedal withdrawal reflex (toe pinch test) and corneal reflex. Terminal blood collection was performed via complete exsanguination from the posterior vena cava (5 mm caudal to renal veins, 22G needle, 30° angle), yielding 3.5 ± 0.3 mL blood per rat (approximately 25–30% total blood volume, based on 6–7% body weight blood volume). Immediately after blood collection, euthanasia was confirmed by bilateral thoracotomy. No animals exhibited signs of distress (e.g., vocalization, escape attempts) during the procedure.

Blood was divided into plain tubes (3 mL, clotted at 4 °C for 30 min, centrifuged at 3000 rpm/1500 ×g for serum ELISA) and EDTA tubes (the remaining volume, immediately centrifuged for plasma storage at –80 °C). Intestinal tissues were sampled as follows: a 0.8 cm segment 5 cm from the ileocecal valve was fixed in 4% PFA for histopathology, and two 200 mg segments 10 cm from the ileocecal valve were snap-frozen in liquid nitrogen (–70 °C) for molecular assays.

Immunohistochemical Detection of CD86 and CD206

Paraffin-embedded sections of intestinal tissue were deparaffinized using xylene and rehydrated through a series of graded ethanol solutions (100%, 95%, 70%, and 50%, each for 5 minutes) before washing with distilled water. Heat-induced antigen retrieval was performed using a pressure cooker or microwave for 15–20 minutes. Endogenous peroxidase activity was quenched by incubating the sections in 3% hydrogen peroxide solution for 10 minutes at room temperature. After blocking with 5% BSA for 30 min, primary antibodies against CD86 (anti-CD86 antibody, dilution 1:200, ab238468, Abcam) and CD206 (anti-CD206 antibody, dilution 1:200, ab64693, Abcam) were applied to the sections overnight at 4 °C in a humidified chamber. On the second day, the sections were washed thoroughly with PBS. The goat anti-rabbit IgG-HRP (31460, Invitrogen, USA) was applied and incubated in a 37 °C incubator for 40 minutes. The sections were then incubated with diaminobenzidine (DAB) substrate solution (Vector Laboratories, USA) for 3–5 minutes under microscopic observation until brown-colored reaction products appeared, indicating positive staining. Hematoxylin was used for counterstaining for 30 seconds to 1 minute, and the slides were rinsed with distilled water. After counterstaining, the slides were dehydrated through a graded series of alcohol (70%, 95%, 100%, each for 5 minutes), cleared with xylene, and cover-slipped. Staining intensity of the brown-yellow granules, indicating positive expression of CD86 and CD206, was measured using a digital image analysis system (Image-Pro Plus or similar software) under a light microscope (e.g., Olympus BX53) (Olympus DP74, USA). The relative protein expression levels were quantified by calculating the mean optical density (MOD) of the positively stained areas.

Histopathological Examination

The excised small intestine was thoroughly rinsed with pre-cooled phosphate-buffered saline (PBS) to remove residual blood and intestinal contents. The tissue was then fixed in 4% paraformaldehyde at 4 °C for 72 hours to preserve its morphological integrity. Following fixation, the tissue was sectioned into smaller fragments, approximately 2–3 mm in thickness, and processed for paraffin embedding. Serial sections of 5-µm thickness were prepared using a microtome and subsequently subjected to hematoxylin and eosin (H&E) staining (Cat. No. 51275 and HT110332, Sigma-Aldrich, USA) for histopathological evaluation.

The stained sections were mounted onto glass slides and sealed with neutral resin. After drying, the slides were examined under a light microscope to assess histological alterations and pathological changes. Quantitative evaluation of intestinal injury was performed using Chiu's scoring system [9], which assesses villous damage, epithelial desquamation, and inflammatory infiltration, providing an objective measure of the extent of intestinal injury under the experimental conditions.

FITC-Dextran Assay

Intestinal permeability was assessed by measuring the flux of fluorescein isothiocyanate-labeled dextran from the intestinal lumen into the systemic circulation. After a 6-hour fast with free access to water, rats were orally gavaged with a sterile solution of FITC-dextran (Sigma-Aldrich, catalog # FD4) dissolved in PBS at a dose of 600 mg/kg. Rats were anesthetized 4 hours post-gavage. Blood was collected via cardiac puncture or from the retro-orbital sinus and placed in heparin-coated microcentrifuge tubes. Plasma was separated by centrifugation at 2000 ×g for 15 minutes at 4 °C. A 50 µL aliquot of plasma from each sample was diluted 1:1 with PBS. The fluorescence intensity of the diluted plasma was measured using a fluorescence microplate reader with an excitation wavelength of 485 nm and an emission wavelength of 535 nm. The concentration of FITC-dextran in each sample was determined by comparison to a standard curve prepared from serial dilutions of the FITC-dextran stock solution in PBS-diluted plasma from an untreated control mouse. Results are expressed as µg/mL of plasma.

Serum D-lactate Levels

Serum D-lactate concentration was quantified using a commercial D-lactate colorimetric assay kit (BioVision, catalog # K667). Briefly, blood samples were collected and allowed to clot at room temperature for 30 minutes. Serum was obtained by centrifugation at 3000 ×g for 15 minutes at 4 °C. For the assay, 50 µL of serum from each sample was added to a 96-well plate, followed by the sequential addition of 100 µL of Reaction Mix and 2 µL of Enzyme Mix. The plate was incubated at 37 °C for 30 minutes, protected from light. The absorbance at 450 nm was measured using a microplate reader. The concentration of D-lactate in each sample was calculated by interpolation from a standard curve generated with known concentrations of D-lactate standard provided in the kit. All samples were assayed in duplicate. Results are expressed as µmol/L or mg/dL of serum.

Western Blotting

Total protein was extracted from small intestinal tissue using RIPA lysis buffer contain in 0.01% PMSF. Equivalent amounts of protein were loaded onto a 12% SDS-PAGE gel for separation. After electrophoresis, the proteins were transferred onto a PVDF membrane via electroblotting. The membrane was blocked at room temperature using 5% non-fat dry milk for 1 hour to minimize non-specific antibody binding. Following blocking, the membrane was incubated overnight at 4 °C with primary antibodies, including anti-p-NFκB (ab76302), anti-TLR4 (ab30667), anti-IκB (ab32518), and GAPDH (ab8245) (1:1000; all antibodies were purchased from Abcam). GAPDH was used as the internal control. The next day, after PBS washing, the membrane was treated with an HRP-conjugated secondary antibody (1:2000, ab6721, Abcam) or HRP-conjugated goat anti-mouse IgG secondary antibody (1:5000, ab205719, Abcam) for 1 hour at room temperature. After three PBS washes, protein detection was carried out using enhanced chemiluminescence (ECL) reagent. ImageJ software (version 1.54, National Institutes of Health, Bethesda, MD, USA) was used to analyze the protein bands and quantify expression levels.

Cell Line and Treatment

Murine macrophage cell line (RAW264.7) cell line was purchased from the Cell Bank of the Chinese Academy of Sciences (Shanghai, China; Catalog No. SCSP-5036). The vendors confirmed that the cells were identified using STR profiling. All cell lines were examined for the presence of mycoplasma using a LookOut® Mycoplasma PCR Detection Kit (Merck & Co., Kenilworth, NJ, USA). The results were negative in all cases, confirming the absence of mycoplasma contamination. Cells were cultured in DMEM complete medium (Thermo Fisher Scientific, China, 8120365) supplemented with 1% penicillin-streptomycin and 10% fetal bovine serum (Thermo Fisher Scientific, China, 2279604CP). The cells were maintained at 37 °C in a humidified incubator with 5% CO_2 and 95% air. The cells were randomly divided into five groups to further explore the therapeutic mechanisms of control (Ctrl), LPS, ESK (100 µmol/L), ESK+TLR4 agonist and TLR4 agonist for 12 h. MPLA (a TLR4 agonist, catalog # tlrl-mpls, InvivoGen) was added to the complete culture medium at a final concentration of 1 µg/mL. Except for the control group, the other four groups of cells before the treatment were treated with LPS solution (from Escherichia coli O111:B4, Sigma-Aldrich, catalog # L2630), which was added to the complete culture medium at a final concentration of 100 ng/mL and incubated at 37 °C with 5% CO_2 for an additional 24 h to induced cell model of sepsis. Subsequently, the ESK, TLR4 agonist and ESK + TLR4 agonist groups were respectively added with ESK (100 µmol/L), MPLA (1 µg/mL, a TLR4 agonist, catalog # tlrl-mpls, InvivoGen) and ESK + TLR4 agonist for 12 h.

Flow Cytometry

Five groups of RAW264.7 cells were seeded in 6-well plates at a concentration of 4×10^5 cells per well and incubated for 48 hours. After incubation, the cells were washed with pre-cooled PBS for 15 minutes and then

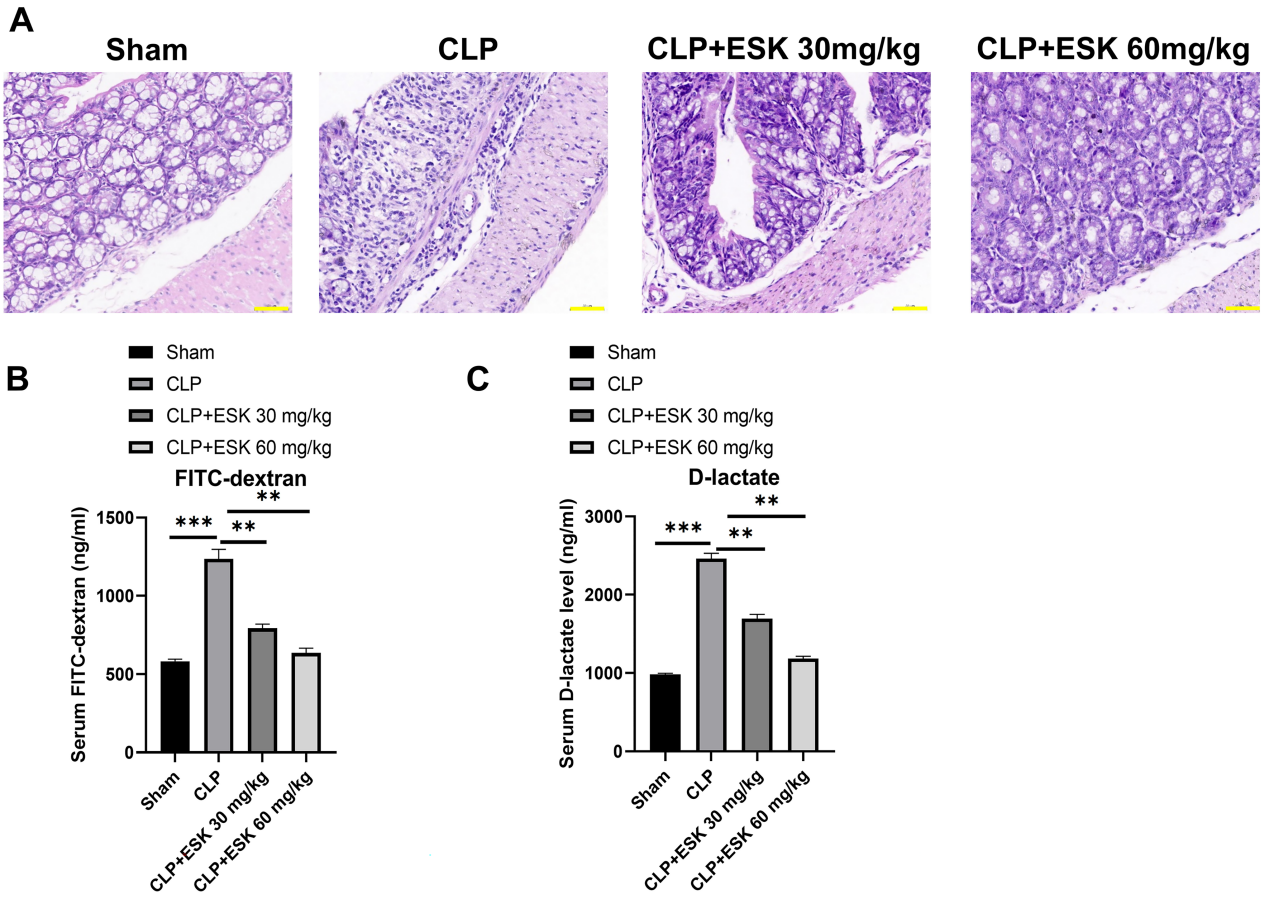

Fig. 1. ESK ameliorates sepsis-induced intestinal injury and improves intestinal permeability. (A) H&E staining analysis of Sepsis-Induced Intestinal Injury of the rats in the Sham, CLP (cecal ligation and puncture), CLP + ESK 30 mg/kg, and CLP + ESK 60 mg/kg groups (scale bar 50 μm). Magnification ×400. (B) Serum levels of FITC-dextran in the Sham, CLP (cecal ligation and puncture), CLP + ESK 30 mg/kg, and CLP + ESK 60 mg/kg groups ($n = 8$). (C) Serum levels of D-lactate in the Sham, CLP (cecal ligation and puncture), CLP + ESK 30 mg/kg, and CLP + ESK 60 mg/kg groups ($n = 8$). $^{**}p < 0.01$, $^{***}p < 0.001$. ESK, Esketamine; H&E, hematoxylin and eosin; FITC, Fluorescein Isothiocyanate.

resuspended in 500 μL of binding buffer. Surface staining was performed using the following antibodies: FITC-conjugated anti-F4/80 (123108, BioLegend, USA), PE-conjugated anti-CD86 (12-0862-82, eBioscience, USA), and APC-conjugated anti-CD206 (141708, BioLegend, USA). Cells were incubated with antibodies for 30 min at 4 °C in the dark. Following staining, cells were washed twice with staining buffer and resuspended in PBS for acquisition. Macrophages were gated as F4/80-positive population, and the percentages of CD86-positive and CD206-positive cells within the $F4/80^+$ gate were quantified. Cells were collected on BD FACSVerseTM (catalog # 556547; BD Biosciences, USA) and analyzed using FlowJo software (Version 10.0, TreeStar, USA).

Statistical Analysis

Statistical analysis was performed using Prism version 22.0 software (GraphPad Software, San Diego, CA, USA). For the four groups of rats, one-way analysis of variance (ANOVA) was applied when the data met the criteria for normal distribution and homogeneity of variance, followed by Tukey's HSD analysis for post hoc multiple-group comparisons. Kaplan-Meier survival analysis was conducted to compare survival rates among the groups.

Results

ESK Ameliorates Sepsis-Induced Intestinal Injury and Improves Intestinal Permeability

To investigate the impact of ESK on sepsis, a rat sepsis model was established using the CLP procedure, excluding the sham group. After the surgery, rats were maintained on a regular diet with or without ESK supplementation for two weeks. Intestinal mucosal damage was subsequently assessed through H&E staining. Fig. 1A displays representative H&E-stained sections from the Sham, CLP, CLP + ESK 30 mg/kg, and CLP + ESK 60 mg/kg groups. The Sham group exhibited normal intestinal architecture,

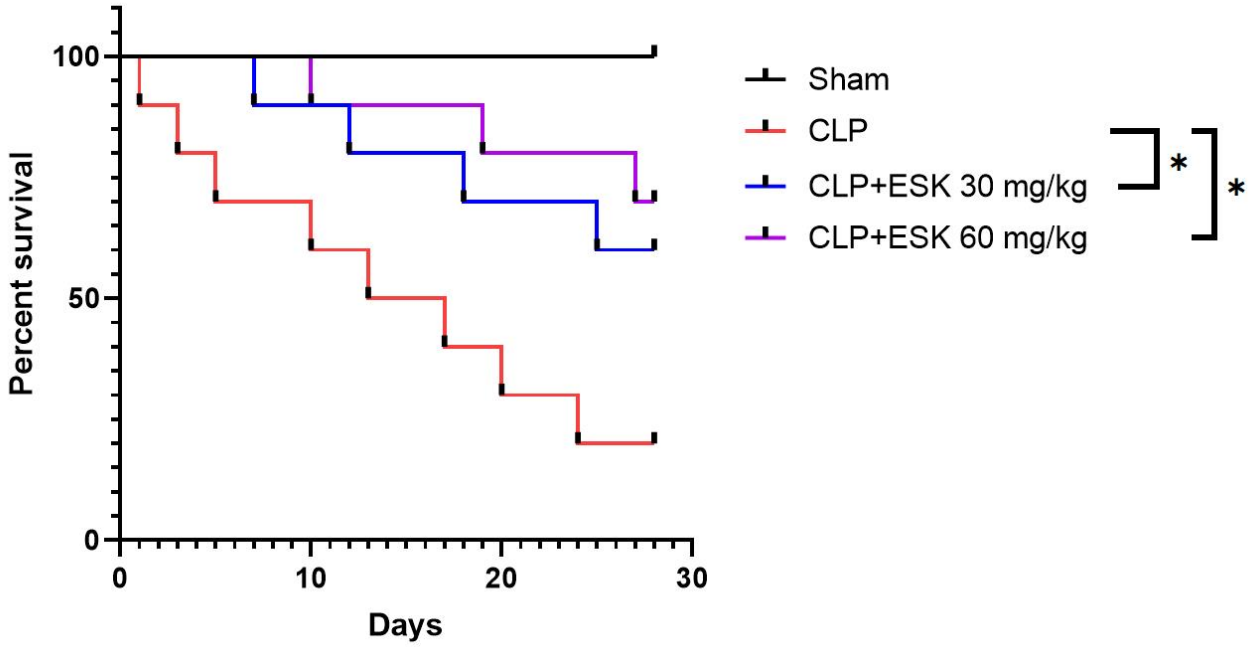

Fig. 2. Effect of ESK on the survival of septic rats. Septic rats (n = 10 for each group) were fed with ESK for 2 weeks. Kaplan-Meier survival curve representing the survival probability of rats over 30 days following cecal ligation and puncture (CLP)-induced sepsis. *$p < 0.05$.

whereas the CLP group presented considerable structural damage, characterized by epithelial disruption and infiltration of inflammatory cells. In contrast, the ESK treatment demonstrated improvement in intestinal structure. Both treatment groups showed a reduction in cell necrosis and a decrease in the number of inflammatory cells, with the 60 mg/kg ESK group approaching nearly normal tissue morphology. Additionally, intestinal barrier integrity was assessed by serum FITC-dextran levels (Fig. 1B). The CLP group showed a significant increase in serum FITC-dextran levels compared to the Sham group ($p < 0.05$), reflecting enhanced intestinal permeability. Notably, ESK treatment led to a decrease in FITC-dextran levels ($p < 0.05$), indicating improvement in barrier function. Furthermore, serum D-lactate levels (Fig. 1C), a marker for bacterial translocation, were significantly elevated in the CLP group, corroborating intestinal barrier dysfunction. ESK treatment significantly lowered D-lactate levels ($p < 0.05$), underscoring its role in preventing bacterial translocation and maintaining intestinal barrier integrity during sepsis.

Behavioral Effects and Survival Benefits of ESK in Septic Rats

In all experimental groups, the sham-operated rats showed no observable abnormal behaviors. However, rats in the sepsis model group exhibited various symptoms, such as curling up, delayed responses, piloerection, diarrhea, fever, and chills within three hours post-surgery. In contrast, the rats treated with ESK exhibited milder symptoms compared to the untreated sepsis group, along with increased levels of activity.

In a separate experiment, the survival rates of ten rats per group were monitored. ESK administration at doses of 30 mg/kg ($p < 0.05$) and 60 mg/kg ($p < 0.05$) significantly improved survival outcomes compared to the untreated CLP group (Fig. 2). A clear effect was observed, with the highest dose of ESK (60 mg/kg) offering the most substantial survival benefit at approximately 70% survival by day 30. The 30 mg/kg group also demonstrated a significant improvement in survival compared to the CLP group, but the effect was less pronounced than in the 60 mg/kg group.

ESK Blockade Attenuates Sepsis-Induced Intestinal Inflammation

Excessive intestinal inflammation and cytokine storms contribute to disrupted intestinal permeability during sepsis. In the CLP group, the levels of pro-inflammatory cytokines IL-6, IL-1β, and TNF-α were significantly ($p < 0.05$) higher than those in the Sham group, whereas the anti-inflammatory cytokine IL-10 was notably reduced ($p < 0.05$), reflecting a heightened inflammatory response (Fig. 3). In contrast, ESK treatment at both 30 mg/kg and 60 mg/kg doses significantly lowered ($p < 0.05$) IL-6, IL-1β, and TNF-α levels, while increasing ($p < 0.05$) IL-10 production, with the 60 mg/kg dose showing

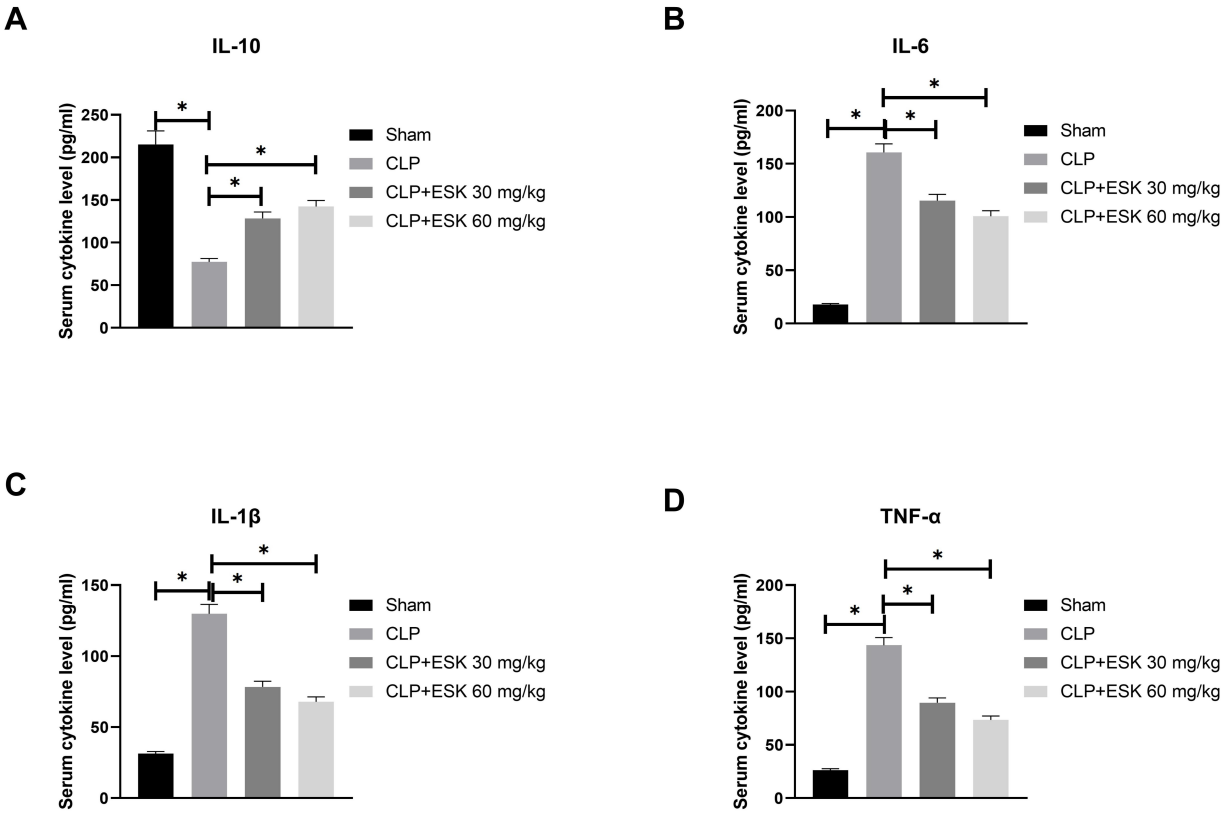

Fig. 3. Effects of ESK on serum cytokine levels in septic rats. The levels of anti-inflammatory (IL-10 (A)) and pro-inflammatory (IL-6 (B), IL-1β (C), TNF-α (D)) cytokines were measured in serum samples from different groups of rats: Sham, CLP, CLP + ESK 30 mg/kg, and CLP + ESK 60 mg/kg ($n = 8$). *$p < 0.05$. IL, Interleukin-1; TNF-α, Tumor Necrosis Factor-alpha.

the most substantial impact. These results indicate that ESK helps reduce systemic inflammation in septic rats.

ESK Induces Macrophage M2 Polarization in Septic Rats

To further investigate whether the anti-sepsis properties of ESK are linked to alterations in macrophage polarization, qPCR and Western blot analyses on intestinal homogenates were conducted, along with IHC assays on frozen intestinal sections to evaluate the expression of genes related to M1 and M2 macrophage polarization. IHC analysis revealed that the CLP group had a marked increase ($p < 0.05$) in CD86-positive M1 macrophages (Fig. 4A–D). ESK treatment counteracted this effect by significantly increasing CD206-positive M2 macrophages ($p < 0.05$). Moreover, mRNA analysis demonstrated that ESK elevated ($p < 0.05$) the levels of anti-inflammatory cytokines IL-10 (Fig. 4E) and Arg1 (an M2 marker) (Fig. 4G) while decreasing ($p < 0.05$) pro-inflammatory markers such as CD86 (Fig. 4F) and iNOS (Fig. 4H). These results suggest that ESK facilitates a transition from M1 to M2 macrophage polarization, thereby reducing inflammation and boosting the anti-inflammatory response in septic rats.

ESK Modulates Macrophage Polarization Through TLR4 Signaling

Building on the previous evidence, we conducted additional *in vitro* experiments to validate the stimulatory effect of ESK on M2 macrophage polarization. The murine macrophage-like cell line RAW 264.7 was treated with LPS to establish an *in vitro* sepsis model, followed by exposure to ESK or a TLR4 agonist. Compared with the LPS group, ESK treatment significantly enhanced ($p < 0.05$) the mRNA expression of anti-inflammatory marker IL-10 (Fig. 5A) and the expression of M2 marker Arg1 (Fig. 5C). while reducing ($p < 0.05$) the levels of M1 marker CD86 (Fig. 5B) and iNOS (Fig. 5D). Co-administration with a TLR4 agonist reversed these effects, suggesting that ESK's influence on macrophage polarization is at least partially mediated through inhibition of the TLR4 pathway. Flow cytometry further corroborated these findings, showing that ESK reduced the proportion of CD86-positive M1 macrophages (Fig. 5E) and increased the proportion of CD206-positive M2 macrophages (Fig. 5F). This effect was partially reversed by the TLR4 agonist, reinforcing the involvement of TLR4 in ESK's regulatory action. Overall, these results demonstrate that ESK promotes a shift towards the anti-inflammatory M2 phenotype while suppressing the

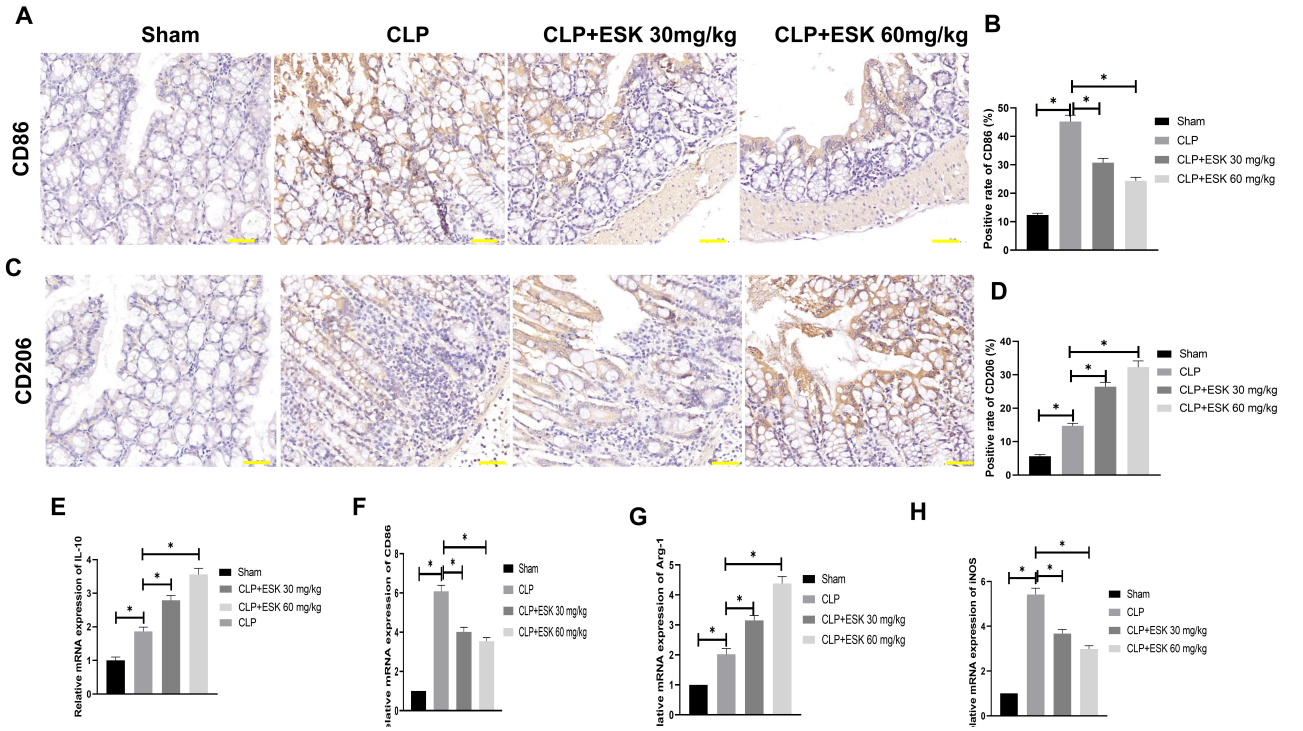

Fig. 4. Effect of ESK (ESK) on macrophage polarization in septic rats. Representative images of CD86 (A,B) and CD206 (C,D) staining in intestinal tissue from each group (scale bar 50 μm). The relative mRNA expression of IL-10 (n = 8). (E) IL-10 (anti-inflammatory cytokine), (F) CD86 (M1 macrophage marker), (G) Arg1 (M2 macrophage marker), and (H) iNOS (M1 macrophage marker) was measured using qRT-PCR (n = 6). *$p < 0.05$.

pro-inflammatory M1 phenotype, with TLR4 signaling being a key component of this mechanism.

ESK Inhibits TLR4/NF-κB Pathway Activation in LPS-Stimulated Macrophages

LPS treatment led to a significant ($p < 0.05$) increase in TLR4 (Fig. 6B) and p-NFκB (Fig. 6C) protein levels, accompanied by a reduction ($p < 0.05$) in IκBα levels (Fig. 6D), indicating activation of the TLR4/NF-κB pathway (Fig. 6A). ESK treatment, however, reduced ($p < 0.05$) the expression of both p-NFκB and TLR4, while restoring IκBα levels, suggesting that ESK inhibits NF-κB activation by preventing IκBα degradation and downregulating TLR4 expression. When co-treated with a TLR4 agonist, these effects were reversed, further supporting the notion that ESK's anti-inflammatory properties are mediated through modulation of the TLR4 signaling pathway.

Discussion

In this study, we demonstrate that ESK protects against sepsis-induced intestinal injury by promoting M2 macrophage polarization while inhibiting M1 macrophage activity. Our findings showed that ESK administration improved intestinal permeability, reduced systemic inflammation, and prolonged survival in a rat model of sepsis. Histological analysis revealed that ESK alleviated intestinal mucosal damage. In addition, ESK treatment significantly reduced serum levels of pro-inflammatory cytokines such as IL-1β, IL-6, and TNF-α, highlighting its role in mitigating systemic inflammatory responses. Further investigation using an *in vitro* model of LPS-induced sepsis in RAW 264.7 macrophages confirmed that ESK modulates macrophage polarization by enhancing M2 markers and suppressing M1 markers, as evidenced by decreased CD86 and increased CD206 expression. This effect was associated with the inhibition of the TLR4/NF-κB signaling pathway, a key mediator of inflammatory responses. Notably, the protective effects of ESK on macrophage polarization were reversed by the co-administration of a TLR4 agonist. A TLR4 siRNA or alternative inhibitors will be employed to indicate that TLR4 plays a pivotal role in ESK's modulation of macrophage activity.

ESK, the S-enantiomer of ketamine, has recently garnered attention for its stronger analgesic effects and reduced psychological side effects compared to ketamine. Clinically, ESK has been widely adopted in perioperative analgesia, pediatric and obstetric anesthesia, endoscopic procedures, and sedation in ICU settings [20,24–26]. Previous studies have shown that ketamine exhibits potent anti-inflammatory and immunomodulatory properties, with sub-anesthetic doses effectively reducing inflammatory cytokine release [4,27–29]. In experimental models of sepsis, ketamine has been shown to reduce mortality and pro-

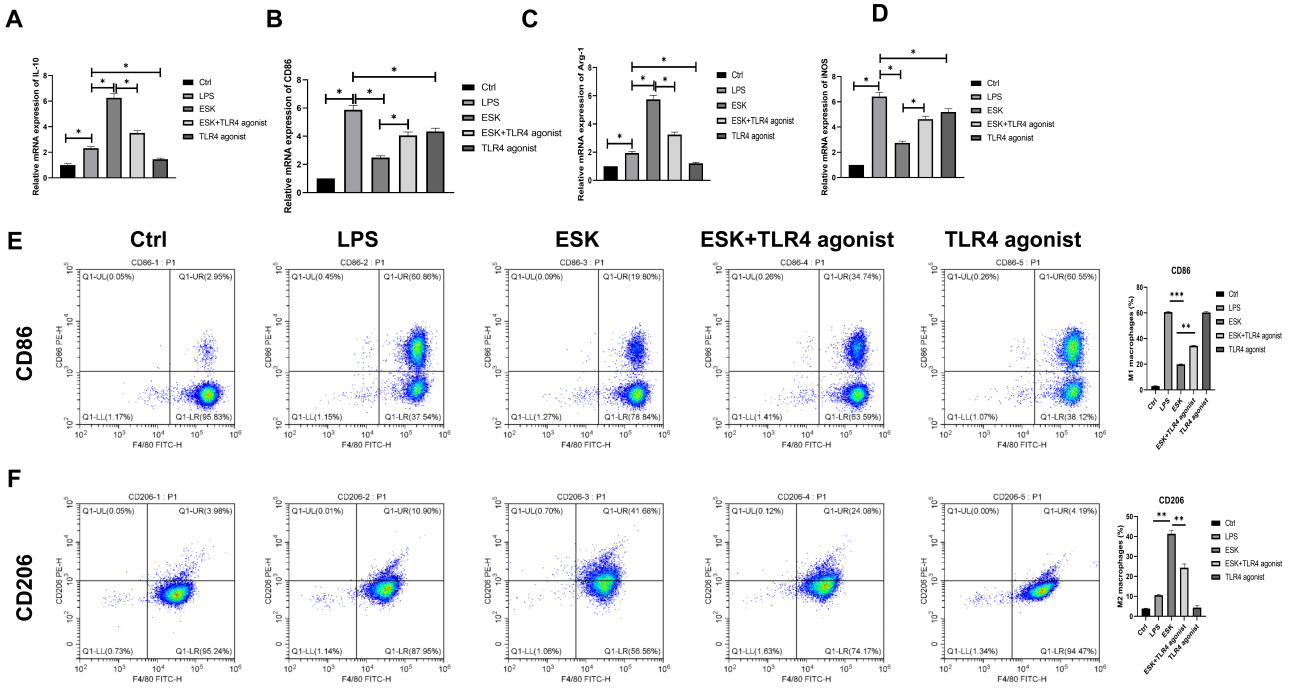

Fig. 5. Effect of ESK (ESK) on pro-inflammatory cytokine levels in LPS-stimulated macrophages. The RAW 264.7 *in vitro* sepsis model was induced with LPS. After that, the RAW 264.7 cells were exposed to ESK/TLR4 agonist. 24 h later, RT-qPCR analysis of IL-10 (A), CD86 (B), Arg-1 (C) and iNOS (D); Expression of CD86 (E) and CD206 (F) was analyzed by flow cytometry ($n = 6$). *$p <$ 0.05, **$p < 0.01$, ***$p < 0.001$. LPS, lipopolysaccharide; TLR, Toll-like receptor.

tect against organ damage, such as endotoxin-induced acute lung injury and myocardial injury, through mechanisms involving the Nrf2/HO-1 signaling pathway [21,22]. Similarly, ESK has been reported to protect against sepsis-induced acute kidney injury in rats. The gastrointestinal tract is often regarded as a "trigger organ" in the progression of sepsis and multiple organ dysfunction syndrome (MODS) [30]. Compared with ordinary ketamine, ESK may have a better anti-inflammatory effect, and it is speculated that it may have a greater advantage in the treatment of sepsis-induced intestinal injury. In our study, ESK effectively ameliorated sepsis-induced intestinal injury and improved the survival of septic rats. Furthermore, ESK reduced serum levels of pro-inflammatory cytokines and promoted M2 macrophage polarization, indicating that ESK maintains the functional integrity of the immune barrier in sepsis. As critical immune cells, macrophages play a key role in both promoting inflammation and facilitating tissue repair. M2 macrophages, in particular, contribute to the resolution of inflammation and the repair of tissue damage, making them essential for sepsis treatment. Our results indicate that ESK promotes macrophage M2 polarization while suppressing the M1 phenotype, suggesting its protective effect on the immune barrier during sepsis.

Toll-like receptors (TLRs), particularly TLR4, are crucial pattern recognition receptors that initiate innate immune responses and link innate and adaptive immunity. Activation of the TLR4/NF-κB pathway is a well-established mechanism in inflammation, driving the production of pro-inflammatory cytokines such as IL-1β, IL-6, and TNF-α [16,17]. These cytokines further amplify the inflammatory cascade, leading to sustained release of inflammatory mediators and the development of systemic inflammatory response syndrome (SIRS) [31–33]. TLR4 is also a key regulator of macrophage polarization, with its activation promoting M1 polarization [34]. Our *in vitro* study confirmed that ESK suppresses TLR4/NF-κB signaling, leading to reduced M1 polarization and enhanced M2 polarization. However, the TLR4 agonist abolished these effects, further supporting the role of TLR4 in mediating ESK's anti-inflammatory and immunomodulatory actions.

However, there were some limitations in this study. Given esketamine's potential to cross the blood-brain barrier and modulate central nervous system (CNS) activity [35], which may indirectly influence intestinal function [36]. Future studies should employ more comprehensive animal models, such as the vagus nerve transection model, to further explore whether the protective effect of ESK against sepsis-induced intestinal injury is partially mediated through the CNS pathways. Moreover, human studies will be designed to validate. However, the lack of long-term survival and histological follow-up prevents conclusions about the durability of ESK's effects. Future studies should assess long-term survival and histological effects.

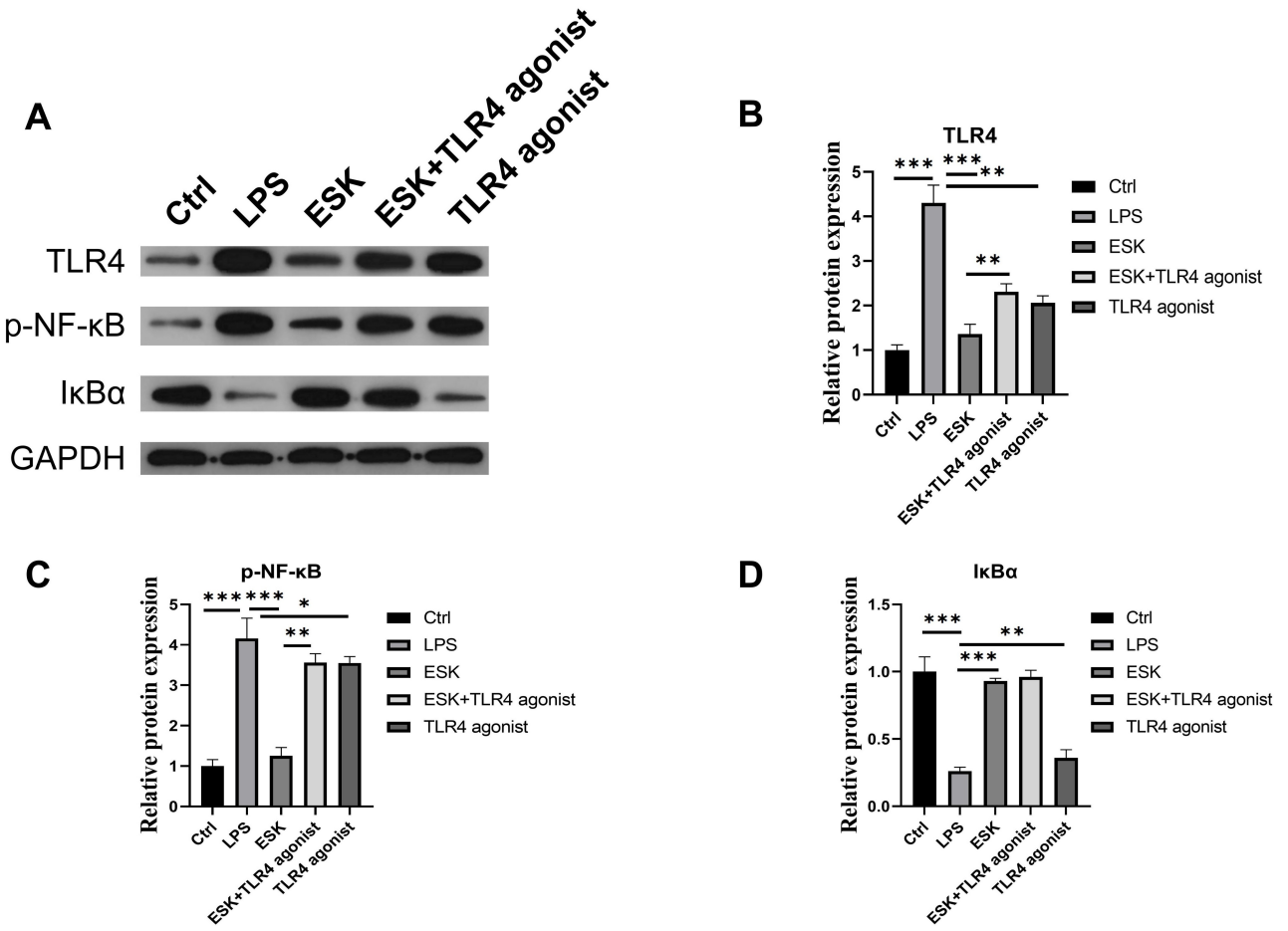

Fig. 6. The RAW 264.7 *in vitro* sepsis model was induced with LPS. After that, the RAW 264.7 cells were exposed to ESK/TLR4 agonist. 24 h later, the levels of TLR4/NF-κB signaling pathway were verified by Western blotting in the supernatants of macrophages from different treatment groups: control (Ctrl), LPS, ESK, ESK + TLR4 agonist, and TLR4 agonist alone (n = 3). (A) Representative images of the TLR4/NFκB signaling pathway, (B) relative protein level of TLR4, (C) relative protein level of p-NF-κB, and (D) relative protein level of IκBα. *$p < 0.05$, **$p < 0.01$, ***$p < 0.001$.

Esketamine is known to modulate multiple signaling pathways, such as HIF-1α/HO-1 pathway [37], which may contribute to its downstream effects. MyD88 is a key signaling adaptor downstream of TLR4 that dominates early inflammatory responses [38]. This mechanism is critical for host defense and regulation of inflammation. ESK has been reported to influence gut microbial function [39]. Small phenolic compounds were also reported to have downstream metabolites that may indirectly affect biological mechanisms [40]. Therefore, we speculate that ESK may regulate sepsis-induced intestinal injury through modulation of gut microbiota, which needs further investigation in future studies. Additionally, we used the established doses to explore the dose-response relationship. However, the optimal therapeutic dose must be determined in future studies. Furthermore, the TLR4 siRNA experiment will be conducted in future studies to strengthen the conclusion at the genetic level. Details of changes in downstream molecular pathways of the TLR4 pathway, for instance, the key adaptor protein MyD88 downstream of TLR4, will be subject to further investigation in future studies.

Conclusion

In conclusion, ESK exerts significant protective effects against sepsis-induced intestinal injury and systemic inflammation, primarily by promoting M2 macrophage polarization and suppressing M1 polarization through the TLR4/NF-κB signaling pathway. These findings suggest that ESK may be a promising therapeutic agent for managing sepsis and reducing organ damage, with its modulation of macrophage polarization playing a central role in its anti-inflammatory and organ-protective effects. Further studies are warranted to explore the potential clinical applications of ESK in sepsis treatment. Further research is required to confirm its efficacy in clinical settings and to investigate the long-term effects of ESK on macrophage polarization and immune homeostasis.

Availability of Data and Materials

The datasets used or analyzed during the current study are available from the corresponding author upon reasonable request.

Author Contributions

LM conceived and designed research; LM conducted the experiments and drafted the manuscript; LZ contributed to data acquisition and critically revised the manuscript; MZ analyzed the data and critically revised the manuscript; QC performed data analysis and interpretation and critically revised the manuscript. All authors have read and approved the final manuscript. All authors have participated sufficiently in the work and agreed to be accountable for all aspects of the work.

Ethics Approval and Consent to Participate

Approval was granted by the Ethics Committee of Fujian Medical University (No. 2023-0131).

Acknowledgment

Not applicable.

Funding

This research is supported by the Startup Fund for scientific research, Fujian Medical University (Grant number: 2022QH1195).

Conflict of Interest

The authors declare no conflict of interest.

References

[1] Gauer R, Forbes D, Boyer N. Sepsis: Diagnosis and Management. American Family Physician. 2020; 101: 409–418.

[2] Vincent JL. Current sepsis therapeutics. EBioMedicine. 2022; 86: 104318. https://doi.org/10.1016/j.ebiom.2022.104318.

[3] Chiu C, Legrand M. Epidemiology of sepsis and septic shock. Current Opinion in Anaesthesiology. 2021; 34: 71–76. https://doi.org/10.1097/ACO.0000000000000958.

[4] Huang M, Cai S, Su J. The Pathogenesis of Sepsis and Potential Therapeutic Targets. International Journal of Molecular Sciences. 2019; 20: 5376. https://doi.org/10.3390/ijms20215376.

[5] Khan N, Kumar V, Li P, RAPIDS Study Group, Schlapbach LJ, Boyd AW, *et al*. Inhibiting Eph/ephrin signaling reduces vascular leak and endothelial cell dysfunction in mice with sepsis. Science Translational Medicine. 2024; 16: eadg5768. https://doi.org/10.1126/scitranslmed.adg5768.

[6] Ling H, Lin Y, Bao W, Xu N, Chen L, Zhao L, *et al*. Erythropoietin-mediated IL-17 F attenuates sepsis-induced gut microbiota dysbiosis and barrier dysfunction. Biomedicine & Pharmacotherapy. 2023; 165: 115072. https://doi.org/10.1016/j.biopha.2023.115072.

[7] Sun J, Zhang J, Wang X, Ji F, Ronco C, Tian J, *et al*. Gut-liver crosstalk in sepsis-induced liver injury. Critical Care (London, England). 2020; 24: 614. https://doi.org/10.1186/s13054-020-03327-1.

[8] Wang Z, Wang Z. The role of macrophages polarization in sepsis-induced acute lung injury. Frontiers in Immunology. 2023; 14: 1209438. https://doi.org/10.3389/fimmu.2023.1209438.

[9] Chiu CJ, McArdle AH, Brown R, Scott HJ, Gurd FN. Intestinal mucosal lesion in low-flow states. I. A morphological, hemodynamic, and metabolic reappraisal. Archives of Surgery (Chicago, Ill.: 1960). 1970; 101: 478–483. https://doi.org/10.1001/archsurg.1970.01340280030009.

[10] Zhu H, Shen F, Liao T, Qian H, Liu Y. Immunosenescence and macrophages: From basics to therapeutics. The International Journal of Biochemistry & Cell Biology. 2023; 165: 106479. https://doi.org/10.1016/j.biocel.2023.106479.

[11] Lai K, Song C, Gao M, Deng Y, Lu Z, Li N, *et al*. Uridine Alleviates Sepsis-Induced Acute Lung Injury by Inhibiting Ferroptosis of Macrophage. International Journal of Molecular Sciences. 2023; 24: 5093. https://doi.org/10.3390/ijms24065093.

[12] Chen R, Cao C, Liu H, Jiang W, Pan R, He H, *et al*. Macrophage Sprouty4 deficiency diminishes sepsis-induced acute lung injury in mice. Redox Biology. 2022; 58: 102513. https://doi.org/10.1016/j.redox.2022.102513.

[13] Chen XS, Wang SH, Liu CY, Gao YL, Meng XL, Wei W, *et al*. Losartan attenuates sepsis-induced cardiomyopathy by regulating macrophage polarization via TLR4-mediated NF-κB and MAPK signaling. Pharmacological Research. 2022; 185: 106473. https://doi.org/10.1016/j.phrs.2022.106473.

[14] Li J, Chen Y, Li R, Zhang X, Chen T, Mei F, *et al*. Gut microbial metabolite hyodeoxycholic acid targets the TLR4/MD2 complex to attenuate inflammation and protect against sepsis. Molecular Therapy: the Journal of the American Society of Gene Therapy. 2023; 31: 1017–1032. https://doi.org/10.1016/j.ymthe.2023.01.018.

[15] Bai Y, Min R, Chen P, Mei S, Deng F, Zheng Z, *et al*. Disulfiram blocks inflammatory TLR4 signaling by targeting MD-2. Proceedings of the National Academy of Sciences of the United States of America. 2023; 120: e2306399120. https://doi.org/10.1073/pnas.2306399120.

[16] Ciesielska A, Matyjek M, Kwiatkowska K. TLR4 and CD14 trafficking and its influence on LPS-induced pro-inflammatory signaling. Cellular and Molecular Life Sciences: CMLS. 2021; 78: 1233–1261. https://doi.org/10.1007/s00018-020-03656-y.

[17] Li Y, Jiang Q, Wang L. Appetite Regulation of TLR4-Induced Inflammatory Signaling. Frontiers in Endocrinology. 2021; 12: 777997. https://doi.org/10.3389/fendo.2021.777997.

[18] Wang JS, Hu Q, Cao RY, Liu WK, Guo ML, Lin Y, *et al*. Progress in the Application of Esketamine During the Perioperative Period. Drug Design, Development and Therapy. 2026; 20: 579462. https://doi.org/10.2147/DDDT.S579462.

[19] Nikayin S, Murphy E, Krystal JH, Wilkinson ST. Long-term safety of ketamine and esketamine in treatment of depression. Expert Opinion on Drug Safety. 2022; 21: 777–787. https://doi.org/10.1080/14740338.2022.2066651.

[20] Feeney A, Papakostas GI. Pharmacotherapy: Ketamine and Esketamine. The Psychiatric Clinics of North America. 2023; 46: 277–290. https://doi.org/10.1016/j.psc.2023.02.003.

[21] Bao Y, Feng Z, Niu Y, Hu Q, Liu H, Zhang H, *et al*. Esketamine mitigates endotoxin-induced acute lung injury by suppressing caspase-11-driven pyroptosis. BMC Anesthesiology. 2025; 25: 356. https://doi.org/10.1186/s12871-025-03220-w.

[22] Li K, Yang J, Han X. Ketamine attenuates sepsis-induced acute lung injury via regulation of HMGB1-RAGE pathways. International Immunopharmacology. 2016; 34: 114–128. https://doi.org/10.1016/j.intimp.2016.01.021.

[23] Zhou X, Li Q, Luo Q, Wang L, Chen J, Xiong Y, *et al*. A single dose of ketamine relieves fentanyl-induced-hyperalgesia by reducing inflammation initiated by the TLR4/NF-κB pathway in rat spinal cord neurons. Drug Discoveries & Therapeutics. 2023; 17: 279–288. https://doi.org/10.5582/ddt.2023.01029.

[24] Jalloh M. Esketamine (Spravato) for Treatment-Resistant Depression. American Family Physician. 2020; 101: 339–340.

[25] Ma S, Dou Y, Wang W, Wei A, Lan M, Liu J, *et al*. Association between esketamine interventions and postpartum depression and analgesia following cesarean delivery: a systematic review and meta-analysis. American Journal of Obstetrics & Gynecology MFM. 2024; 6: 101241. https://doi.org/10.1016/j.ajogmf.2023.101241.

[26] Swainson J, Thomas RK, Archer S, Chrenek C, MacKay MA, Baker G, *et al*. Esketamine for treatment resistant depression. Expert Review of Neurotherapeutics. 2019; 19: 899–911. https://doi.org/10.1080/14737175.2019.1640604.

[27] Dai J, Li S, Zheng R, Li J. Effect of esketamine on inflammatory factors in opioid-free anesthesia based on quadratus lumborum block: A randomized trial. Medicine. 2023; 102: e34975. https://doi.org/10.1097/MD.0000000000034975.

[28] Qiu D, Wang XM, Yang JJ, Chen S, Yue CB, Hashimoto K, *et al*. Effect of Intraoperative Esketamine Infusion on Postoperative Sleep Disturbance After Gynecological Laparoscopy: A Randomized Clinical Trial. JAMA Network Open. 2022; 5: e2244514. https://doi.org/10.1001/jamanetworkopen.2022.44514.

[29] Wang T, Weng H, Zhou H, Yang Z, Tian Z, Xi B, *et al*. Esketamine alleviates postoperative depression-like behavior through anti-inflammatory actions in mouse prefrontal cortex. Journal of Affective Disorders. 2022; 307: 97–107. https://doi.org/10.1016/j.jad.2022.03.072.

[30] Yao AJ, Leng YF. Effects of ketamine on renal ischemia-reperfusion injury in rats. Chinese Journal of Anesthesiology. 2009; 29: 927–931. (In Chinese)

[31] Juskewitch JE, Platt JL, Knudsen BE, Knutson KL, Brunn GJ, Grande JP. Disparate roles of marrow- and parenchymal cell-derived TLR4 signaling in murine LPS-induced systemic inflammation. Scientific Reports. 2012; 2: 918. https://doi.org/10.1038/srep00918.

[32] Qi-Xiang M, Yang F, Ze-Hua H, Nuo-Ming Y, Rui-Long W, Bin-Qiang X, *et al*. Intestinal TLR4 deletion exacerbates acute pancreatitis through gut microbiota dysbiosis and Paneth cells deficiency. Gut Microbes. 2022; 14: 2112882. https://doi.org/10.1080/19490976.2022.2112882.

[33] Yang K, Fan M, Wang X, Xu J, Wang Y, Tu F, *et al*. Lactate promotes macrophage HMGB1 lactylation, acetylation, and exosomal release in polymicrobial sepsis. Cell Death and Differentiation. 2022; 29: 133–146. https://doi.org/10.1038/s41418-021-00841-9.

[34] Olona A, Hateley C, Muralidharan S, Wenk MR, Torta F, Behmoaras J. Sphingolipid metabolism during Toll-like receptor 4 (TLR4)-mediated macrophage activation. British Journal of Pharmacology. 2021; 178: 4575–4587. https://doi.org/10.1111/bph.15642.

[35] Xu HJ, Li XP, Han LY. Role and mechanism of esketamine in improving postoperative cognitive dysfunction in aged mice through the TLR4/MyD88/p38 MAPK pathway. The Kaohsiung Journal of Medical Sciences. 2024; 40: 63–73. https://doi.org/10.1002/kjm2.12778.

[36] Zhang Y, Ma W, Lin H, Gu X, Xie H. The effects of esketamine on the intestinal microenvironment and intestinal microbiota in mice. Human & Experimental Toxicology. 2023; 42: 9603271231211894. https://doi.org/10.1177/09603271231211894.

[37] Shi J, Song S, Wang Y, Wu K, Liang G, Wang A, *et al*. Esketamine alleviates ferroptosis-mediated acute lung injury by modulating the HIF-1α/HO-1 pathway. International Immunopharmacology. 2024; 142: 113065. https://doi.org/10.1016/j.intimp.2024.113065.

[38] Zhou S, Wang G, Zhang W. Effect of TLR4/MyD88 signaling pathway on sepsis-associated acute respiratory distress syndrome in rats, via regulation of macrophage activation and inflammatory response. Experimental and Therapeutic Medicine. 2018; 15: 3376–3384. https://doi.org/10.3892/etm.2018.5815.

[39] Wu Y, Zhang Y, Xie B, Zhang X, Wang G, Yuan S. Esketamine mitigates cognitive impairment following exposure to LPS by modulating the intestinal flora/subdiaphragmatic vagus nerve/spleen axis. International Immunopharmacology. 2024; 126: 111284. https://doi.org/10.1016/j.intimp.2023.111284.

[40] Tian B, Ye P, Zhou X, Hu J, Wang P, Cai M, *et al*. Gallic Acid Ameliorated Chronic DSS-Induced Colitis Through Gut Microbiota Modulation, Intestinal Barrier Improvement, and Inflammation. Molecular Nutrition & Food Research. 2025; 69: e70024. https://doi.org/10.1002/mnfr.70024.